Narrow-Band Matching Networks for Quasi-TEM Coupled Microstrip Lines

Josh G. Nickel, *Student Member, IEEE*, Mark D. Hampson, Ho-Young R. Chung, and José E. Schutt-Ainé, *Senior Member, IEEE*

***Abstract*—For coupled-line systems, "matching" involves entire impedance matrix networks and necessarily involves multiple propagating modes. This paper presents the synthesis of several matching strategies for symmetric coupled-line microstrip structures mismatched with several types of simple passive terminations. Detailed multiconductor transmission-line analysis provides the basis for procedures to optimize the parameters of several matching networks (stubs, reactances, transformers) that yield significant line and mode reflection reduction resulting from the mismatches. Measurement of synthesized structures verifies the reflection reduction and power savings.**

***Index Terms*—Coupled microstrip, matching networks, multiconductor transmission lines.**

I. Introduction

MUCH literature has addressed quasi-TEM propagation in multiconductor transmission line (MTL) systems [1]–[12]. Faster signals, smaller traces, and increasingly compact packaging are increasing the importance of this analysis. Full-wave electromagnetic (EM) descriptions of coupled transmission-line systems is also a major topic in computational electromagnetics and microwave research, especially for high-frequency microwave applications where discontinuities and radiation become significant.

However, little has been presented regarding general matching strategies for coupled microstrip given mismatched MTL terminations. Ponchak and Katehi [13] applied tuning stub matching to coplanar-waveguide systems on silicon. Kuo and Tzuang [4] reduced reflections using matched termination networks on six-line closely coupled microstrip circuits. Amari and Bornemann [5] minimized reflected power numerically by determining an optimum resistive termination based on random and deterministic source excitations. Sun [11] presented a multiconductor quarter-wave transformer.

In this paper, we synthesize several types of matching networks for symmetric mismatched terminations in symmetric, uniform, and coupled-line microstrip structures in the quasi-TEM regime. Employing MTL theory, stubs, reactive elements, and transformers will be applied to coupled-line systems. Reasonable engineering approximations are utilized in simulation and measurement where necessary, and the matching methods will be applied to a coupled three-line system to exemplify matching for general n-line applications. These may include transistor amplifier circuits substituting microstrip for coplanar technology, opto-electronics packaging, chip- and package-level interconnections, and parallel data buses.

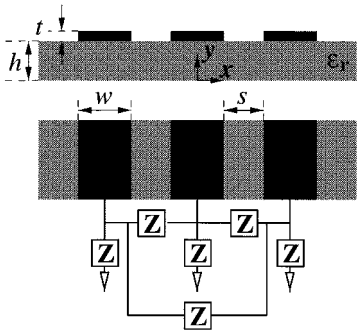

Fig. 1. Cross-sectional and top view of microstrip structure showing dimensions and geometries. An arbitrary complex load is assumed with the Z network.

This paper is organized as follows. In Section II, we overview necessary MTL longitudinal relations. In Section III, we present several matching strategies. In Section IV, numerical results and simulations of the synthesized matching networks are presented. Finally, the matching is validated with measurement results presented in Section V.

II. MTL Equations

Focusing on the microstrip structure shown in Fig. 1, throughout this paper we assume symmetry about the $x = 0$ plane and generalize the results to n lines (excluding the ground plane) where possible.

Under the quasi-TEM approximation, the propagating modes are interpreted as physical system voltages and currents [1]. The wave equations are solved with a linear transformation and change of variables (between conductor and mode) given by the relations [7]

$$\boldsymbol{v}_{\mathrm{m}}(z) = \boldsymbol{E}\boldsymbol{v}_{\mathrm{c}}(z) \tag{1a}$$

$$\boldsymbol{i}_{\mathrm{m}}(z) = \boldsymbol{H}\boldsymbol{i}_{\mathrm{c}}(z) \tag{1b}$$

where $\boldsymbol{E}$ and $\boldsymbol{H}$ are $(n \times n)$ matrices whose ith rows are the voltage and current transformation vectors associated with the

Manuscript received September 17, 1999; revised May 10, 2001.

J. G. Nickel was with the Center for Computational Electromagnetics, University of Illinois at Urbana-Champaign, Urbana, IL 61801 USA. He is now with Silicon Bandwidth Inc., Fremont, CA 94538 USA.

M. D. Hampson and J. E. Schutt-Ainé are with the Center for Computational Electromagnetics, University of Illinois at Urbana-Champaign, Urbana, IL 61801 USA (e-mail: jose@decwa.ece.uiuc.edu).

H.-Y. R. Chung was with the Center for Computational Electromagnetics, University of Illinois at Urbana-Champaign, Urbana, IL 61801 USA. He is now with Raytheon Inc., El Segundo, CA 90245 USA.

Publisher Item Identifier S 0018-9480(02)04051-6.

0018-9480/02$17.00 © 2002 IEEE

ith mode. Transformations $\boldsymbol{E}$ and $\boldsymbol{H}$ must simultaneously diagonalize both the distributed impedance and admittance matrices $\boldsymbol{Z}$ and $\boldsymbol{Y}$ [2] to uncouple the MTL equations, and must obviously be nonsingular [2], [8] to enable transformation between modal and conductor variables. The n column vectors $\boldsymbol{v}_{\rm m}$ and $\boldsymbol{i}_{\rm m}$ are the modal voltage and current vectors that relate to the electric- and magnetic-field configurations for the n modes.

Decoupling the MTL equations yields

$$\boldsymbol{EZYE}^{-1} = \boldsymbol{HYZH}^{-1} = \boldsymbol{\Lambda}_{\rm m}^2 \tag{2}$$

where $\boldsymbol{\Lambda}_{\rm m}^2$ is the (diagonal) eigenvalue matrix for $\boldsymbol{ZY}$ and $\boldsymbol{YZ}$. Matrix $\boldsymbol{\Lambda}_{\rm m}$ contains the ordered complex propagation constants $\gamma_{i=1,2,...,n}$ for modes $i = 1, 2, \ldots, n$. Inhomogeneous media (microstrip) generally yields n distinct eigenvalues [1] resulting in *mode delays* [14]. We easily solve (2) using numerical eigenvalue routines.

The conductor characteristic impedance and admittance matrices $\boldsymbol{Z}_{\rm ch}^{\rm c}$ and $\boldsymbol{Y}_{\rm ch}^{\rm c}$ for the system are

$$\boldsymbol{Z}_{\rm ch}^{\rm c} = \boldsymbol{E}^{-1}\boldsymbol{\Lambda}_{\rm m}^{-1}\boldsymbol{EZ} \Longleftrightarrow \boldsymbol{Y}_{\rm ch}^{\rm c} = \boldsymbol{Z}^{-1}\boldsymbol{E}^{-1}\boldsymbol{\Lambda}_{\rm m}\boldsymbol{E} \tag{3}$$

which agree with [6], [8], and [9] when $\boldsymbol{Z}$, the distributed impedance, is replaced with $j\omega\boldsymbol{L}$, where $\boldsymbol{L}$ is the distributed inductance for the lossless case.

The $(n \times n)$-mode reflection coefficient matrix is

$$\boldsymbol{\Gamma}_{\rm L}^{\rm m} = \left[\boldsymbol{\Lambda}_{\rm m} + \boldsymbol{EZY}_{\rm L}^{\rm c}\boldsymbol{E}^{-1}\right]^{-1}\left[\boldsymbol{\Lambda}_{\rm m} - \boldsymbol{EZY}_{\rm L}^{\rm c}\boldsymbol{E}^{-1}\right]. \tag{4}$$

Correspondingly, the conductor reflection-coefficient matrix that relates forward- and backward-traveling conductor voltages $\boldsymbol{v}^+$ and $\boldsymbol{v}^-$ is shown by definition to be

$$\boldsymbol{\Gamma}_{\rm L}^{\rm c} = \boldsymbol{E}^{-1}\boldsymbol{\Gamma}_{\rm L}^{\rm m}\boldsymbol{E} \tag{5}$$

where c denotes the *conductor*.

The longitudinal input conductor reflection coefficient matrix is [15]

$$\boldsymbol{\Gamma}_{\rm in}^{\rm c}(z) = \boldsymbol{E}^{-1}\boldsymbol{Q}(z)\boldsymbol{\Gamma}_{\rm L}^{\rm m}\boldsymbol{Q}(z)\boldsymbol{E} \tag{6}$$

and is related to the longitudinal input admittance matrix

$$\boldsymbol{Y}_{\rm in}^{\rm c}(z) = \boldsymbol{Y}_{\rm ch}^{\rm c}\left[\boldsymbol{1}_n + \boldsymbol{\Gamma}_{\rm in}^{\rm c}(z)\right]^{-1}\left[\boldsymbol{1}_n - \boldsymbol{\Gamma}_{\rm in}^{\rm c}(z)\right] \tag{7}$$

where $\boldsymbol{1}_n$ is the $(n \times n)$ identity matrix.

III. Matching Strategies

We define *unilateral matching* as matching $\boldsymbol{Y}_{\rm in}^{\rm c}$ to the characteristic admittance matrix $\boldsymbol{Y}_{\rm ch}^{\rm c}$ of the lines, in essence, disregarding the source. *Bilateral matching* accounts for the source and considers the output admittance matrix $\boldsymbol{Y}_{\rm out}^{\rm c}$ looking toward the source conjugately matched to $\boldsymbol{Y}_{\rm in}^{\rm c}$ for some point a, i.e., $[\boldsymbol{Y}_{\rm in}^{\rm c}(z=-d)] = [\boldsymbol{Y}_{\rm out}^{\rm c}(z=-d)]^*$. For $n > 2$, exact matching becomes impractical, especially when the termination is limited to nearest neighbor mutual impedances. For loose coupling, the nonadjacent mutual admittance is negligible, though increasing frequencies, more compact packaging, and complex terminations will result in significant mismatches. We now present some approximate matching strategies for certain conditions.

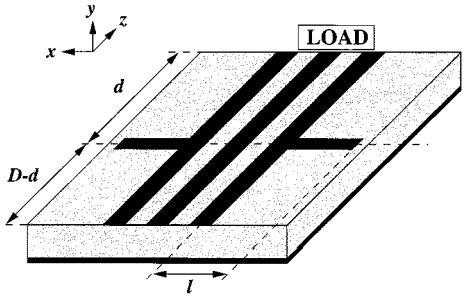

Fig. 2. Coupled three-line system with load plane ($z = 0$) and tuning stubs.

Ideally, a "match" entails maximizing power transfer to the load. In this study, voltage–wave matching will only approximate this ideal since multiple propagating modes with distinct phase velocities give rise to wavelength ambiguities. Consequently, we will start from the given excitation, as per [5], and will determine the dominant mode to match. For moderate coupling, a signal composed of multiple modes can be well matched for short lengths since the mode velocities are relatively similar. Though the unilateral voltage–wave MTL matching to be considered here constitutes a limited set of real-world problems, it will provide a rudimentary conceptual framework for more general MTL matching synthesis.

A. Tuning Stub Application to Simple Mismatches

First, we consider applying open-circuited shunt stubs on the outside lines (1, n) when the impedance between the outside lines and ground is mismatched at the load compared to the characteristic impedance. To elucidate this mismatch more clearly, we resort to the so-called "network impedance matrix" notation of [14] and [15]. This matrix is a compact physical description of an $(n+1)$-terminal network where the ij entry represents the impedance interconnecting nodes i and j when $i \neq j$ or i to ground when $i = j$. For example, the load network is given by $\boldsymbol{\mathcal{Z}}_{\rm L}$. The conductor characteristic impedance matrix $\boldsymbol{Z}_{\rm ch}^{\rm c}$, if realized as a load for a perfect unilateral match, would be $\boldsymbol{\mathcal{Z}}_{\rm ch}$, where $[\boldsymbol{Z}_{\rm ch}^{\rm c}]_{ij} \neq [\boldsymbol{\mathcal{Z}}_{\rm ch}]_{ij}$ in general. Thus, this outside line mismatch is easily written as $[\boldsymbol{\mathcal{Z}}_{\rm L}]_{11,nn} \neq [\boldsymbol{\mathcal{Z}}_{\rm ch}]_{11,nn}$.

To match lines 1 and 3 using shunt stubs, we shift $\boldsymbol{Y}_{\rm in}^{\rm c}(z)$ toward the generator to a distance $z = -d$ such that

$$\Re{\rm e}\left\{\left[\boldsymbol{Y}_{\rm in}^{\rm c}\right]_{11}\right\} = \left[\boldsymbol{Y}_{\rm ch}^{\rm c}\right]_{11}. \tag{8}$$

On a Smith chart, this corresponds to the intersection of the phase-shifted reflection coefficient and the $1 + jX$ circle, provided the source impedance approximately equals the characteristic impedance (in practice, the designers may have flexibility in choosing $\boldsymbol{Y}_{\rm S}^{\rm c}$, and could choose $\boldsymbol{Y}_{\rm S}^{\rm c} = \boldsymbol{Y}_{\rm ch}^{\rm c}$ to approximate bilateral matching if possible). Fig. 2 shows stub parameters in a coupled three-line microstrip.

We assume that the stubs do not couple to the interior lines. Their reference admittance is then the self-characteristic admittance of line 1 or n to ground as if they were isolated. We define this reference admittance $Y_0 = [\boldsymbol{Y}_{\rm ch}^{\rm c}]_{11} + [\boldsymbol{Y}_{\rm ch}^{\rm c}]_{12} + [\boldsymbol{Y}_{\rm ch}^{\rm c}]_{13}$.

Reactive cancellation is achieved if the normalized stub susceptance is

$$B = -j\frac{\Im\mathrm{m}\left\{\left[\boldsymbol{Y}^{\mathrm{c}}_{\mathrm{in}}(z)\right]_{11}\right\}}{\Re\mathrm{e}\{Y_0\}} \tag{9}$$

where we have made the substitution $B = -jX$; the reflection coefficient of the stub is thus

$$\Gamma_{\mathrm{stub}} = -\frac{1-B}{1+B} = |\Gamma_{\mathrm{stub}}|e^{j\phi_{\mathrm{stub}}}. \tag{10}$$

Stub length should be chosen to yield a susceptance to ground of $-\Im\mathrm{m}\{[\boldsymbol{Y}^{\mathrm{c}}_{\mathrm{in}}(-d)]_{11}\}$. This calculation should utilize the propagation velocity of the dominant mode i, i.e.,

$$l = -\frac{\pi - \phi_{\mathrm{stub}}}{2\cdot\Im\mathrm{m}\left\{\left[\boldsymbol{\Lambda}_{\mathrm{m}}\right]_{ii}\right\}}. \tag{11}$$

Now, the input admittance of lines 1 and 3 is modified to include the denormalized stub susceptance

$$\left[\boldsymbol{Y}^{\mathrm{c}}_{\mathrm{in}}(-d)\right]'_{11,\,33} = \left[\boldsymbol{Y}^{\mathrm{c}}_{\mathrm{in}}(-d)\right]_{11} + B(Y_0) \tag{12}$$

so that the stub's reactance cancels the imaginary parts of $[\boldsymbol{Y}^{\mathrm{c}}_{\mathrm{in}}(-d)]_{11,\,nn}$.

Again, we reiterate that this unilateral match cannot provide an exact match unless $\boldsymbol{Y}^{\mathrm{c}}_{\mathrm{S}} = \boldsymbol{Y}^{\mathrm{c}}_{\mathrm{ch}}$. Approximate matching is attained if $\boldsymbol{Y}^{\mathrm{c}}_{\mathrm{S}} \approx \boldsymbol{Y}^{\mathrm{c}}_{\mathrm{ch}}$. If $\boldsymbol{Y}^{\mathrm{c}}_{\mathrm{S}}$ has zero-valued mutual elements (e.g., independent Thevenin excitations), but diagonal elements $[\boldsymbol{Z}^{\mathrm{c}}_{\mathrm{S}}]_{ii} \approx [\boldsymbol{Z}^{\mathrm{c}}_{\mathrm{ch}}]_{ii}$, a good approximate match still results in the moderately coupled microstrip, where self admittances are usually an order of magnitude larger than the mutual admittances

$$\Im\mathrm{m}\{Y_{\mathrm{self}}(z)\} \gg -\Im\mathrm{m}\left\{\left[\boldsymbol{Y}^{\mathrm{c}}_{\mathrm{in}}(z)\right]_{ij}\right\} \tag{13}$$

where the self-admittance of line 1 and n, like the reference admittance, is defined as the sum of the first or last row or column $Y_{\mathrm{self}}(-d) = [\boldsymbol{Y}^{\mathrm{c}}_{\mathrm{in}}(-d)]_{11} + [\boldsymbol{Y}^{\mathrm{c}}_{\mathrm{in}}(-d)]_{12} + [\boldsymbol{Y}^{\mathrm{c}}_{\mathrm{in}}(-d)]_{13} + \cdots$. For extremely tight coupling, the mutual admittances will be much more significant, and this approximation will be worse. Still, almost perfect practical stub matching results for these simple mismatches.

B. Matching Mutual Admittance With Interline Reactance

Our strategy must be expanded to account for symmetric mutual interline mismatches at the load ($[\boldsymbol{Y}^{\mathrm{c}}_{\mathrm{L}}]_{ij} \neq -[\boldsymbol{Y}^{\mathrm{c}}_{\mathrm{S}}]_{ij}$) and mismatches on $[\boldsymbol{Y}^{\mathrm{c}}_{\mathrm{in}}(z)]_{22,\,33,\,\ldots,(n-1)(n-1)}$. We will consider only mutual nearest neighbor mismatches between lines. Perpendicular shunt stubs are clearly impractical for the inside lines. Parallel stubs implemented in coplanar waveguide [13] are difficult to simulate and exceed our interest in simplicity. A lumped reactive element would enable similar susceptance cancellation. Chip capacitors, microstrip gap capacitors, or variable-width trace inductance may be easily placed between mutually mismatched lines at an optimal distance $z = -d$ such that reactive cancellation occurs in one or more off-diagonal term $[Y^{\mathrm{c}}_{\mathrm{in}}(z)]_{ij}$.

We may numerically optimize d (starting with initial guesses in terms of fractions of wavelength) for

$$\Re\mathrm{e}\left\{\left[\boldsymbol{Y}^{\mathrm{c}}_{\mathrm{in}}(z=-d)\right]_{ij}\right\} = -\left[\boldsymbol{Y}^{\mathrm{c}}_{\mathrm{S}}\right]_{ij}. \tag{14}$$

The reactance at $z = -d$ may be canceled with inductance or capacitance. A positive susceptance for $\boldsymbol{Y}^{\mathrm{c}}_{\mathrm{in}}(z=-d)$ implies inductive mismatch, which is cancelled with a capacitance determined by $\Im\mathrm{m}\{Y_{\mathrm{mut}}(-d)\} = \omega C$ at the desired frequency ω. Otherwise, inductance determined by $\Im\mathrm{m}\{Y_{\mathrm{mut}}(-d)\} = (\omega C)^{-1}$ cancels negative susceptance at $z = -d$ and matches the conductances. Matching via chip capacitance is restricted by discrete values and limited by three-dimensional discontinuities; matching via trace inductance is restricted by the line separation s (though the width is variable), and frequency-dependent field effects.

Note again that (14) depends on the source impedance. Assuming that the distance $D-d$ (for reactance matching) is on the order of one half-wavelength or less, our choice of $\boldsymbol{Y}^{\mathrm{c}}_{\mathrm{S}} \approx \boldsymbol{Y}^{\mathrm{c}}_{\mathrm{ch}}$ yields an output admittance that is approximately the characteristic admittance $\boldsymbol{Y}^{\mathrm{c}}_{\mathrm{out}}(z=-d) \approx \boldsymbol{Y}^{\mathrm{c}}_{\mathrm{ch}}$.

A "center tune" reactive cancellation to match $[Y^{\mathrm{c}}_{\mathrm{in}}(z)]_{22,\,33,\,\ldots,(n-1)(n-1)}$ is found for some $z = -d$ where

$$\Re\mathrm{e}\left\{\left[\boldsymbol{Y}^{\mathrm{c}}_{\mathrm{in}}(z)\right]_{22,\,\ldots,(n-1)(n-1)}\right\} = \left[\boldsymbol{Y}_{\mathrm{S}}\right]_{22,\,\ldots,(n-1)(n-1)}. \tag{15}$$

For the three-line case with high impedance from line 2 to ground, we will show that this results in superior matching compared to simple interline reactive cancellation (14).

Finally, for next-neighbor matching where low-impedance terminations "short" the high characteristic mutual admittance, inductive air bridges or wire bonds may be necessary. We leave this synthesis problem for future work.

C. The Quarter-Wave Transformer for Coupled Lines

Sun [11] examined the multiline quarter-wave transformer with two uniformly coupled lines in homogenous media and derived impedance/admittance transformations using the load reflection coefficients and propagation constant matrices. A quarter-wavelength of coupled line with admittance matrix $\boldsymbol{Y}_{\mathrm{q}}$ and terminated by $\boldsymbol{Y}_{\mathrm{L}}$ is attached to the $\boldsymbol{Y}_0$ input section. The input admittance matrix looking into the quarter-wave section toward the load is equated to $\boldsymbol{Y}_0$, and the solution obtained is

$$\boldsymbol{Y}_{\mathrm{L}} = \boldsymbol{Y}_{\mathrm{q}}\boldsymbol{Z}_0\boldsymbol{Y}_{\mathrm{q}}. \tag{16}$$

Sun does not address multiple propagation constants; we will design using the dominant mode.

Practical feasibility of this transformer is clearly limited by planar geometry. Furthermore, optimization will require expensive iterated circuit parameter extraction for the quarter-wave section. However, for certain cases, the transformer may match reasonably well and can be easily fabricated. An example is presented in Section IV.

IV. Numerical Results

We now present results from numerical matching simulations performed on a tightly coupled three-line microstrip structure

(as in Fig. 1) with dimensions $t = 34.29$ μm, $h = 1.50$ mm, $s = 1.0$ mm, and $w = 2.6$ mm and permittivity $\epsilon_r = 4.7$. Electrical parameters were extracted using a quasi-static moment-method ***RLGC*** tool [16]. Parameters $\boldsymbol{R}$ and $\boldsymbol{G}$ were considered negligible given the relatively short lengths of line and high coupling planned for the experiment. Matrices $\boldsymbol{L}$ and $\boldsymbol{C}$ for the microstrip were designed for 50-Ω elements in the diagonal of matrix $\boldsymbol{Z}_{\rm ch}^{\rm c}$ to approximately match the reference impedance. The MTL analysis was numerically implemented in computer code and we optimized the matching parameters $z = -d$ for (8), (14), and (15) using a quasi-Newton scheme.

For the outer line mismatch, two simple cases are examined. The first considers lines 1 and 3 terminated at the load ($z = 0$) by an "open" (430 Ω) to ground ($[\boldsymbol{\mathcal{Z}}_{\rm L}]_{11,\,33} = 430\ \Omega$). In the second case, lines 1 and 3 are terminated by a "short" (20 Ω) to ground ($[\boldsymbol{\mathcal{Z}}_{\rm L}]_{11,\,33} = 20\ \Omega$). In both cases, line 2 is terminated with the inverse self-characteristic admittance $[\boldsymbol{\mathcal{Z}}_{\rm L}]_{22} = \Re\mathrm{e}\{[\boldsymbol{\mathcal{Z}}_{\rm ch}]_{22}\} \approx 69\ \Omega$, and all remaining mutual terminations are matched to the characteristic admittances ($[\boldsymbol{\mathcal{Z}}_{\rm L}]_{ij} = \Re\mathrm{e}\{[\boldsymbol{\mathcal{Z}}_{\rm ch}]_{ij}\}$). While difficult to implement practically, these simple mismatches are easily stub-corrected and demonstrate the validity of the matching network.

Matching parameters d and l were optimized for a design frequency of 2.0 GHz in both cases. The T-junction was modeled using three series inductors of 0.1 nH and a shunt capacitor of 0.2 pF; the open-circuited stub was modeled using an equivalent end-effect approximation [17]. For the given geometry, an end-effect length was approximated as 0.57 mm, or a capacitance of 2.3 pF.

With the mismatch, matrix $\boldsymbol{\Gamma}_{\rm L}^{\rm c}$ had large magnitudes of self-reflections on lines 1 and 3, while reflections into line 1 from lines 2 and 3 were minimal; no forward waves on line 2 were reflected (column 2 all zero). Given that line 2 is matched to ground and lines 1 and 3, this result is physically intuitive, and a zero column is possible since conductor reflection-coefficient matrices are generally asymmetric [2], even for symmetric terminations.

Initial guesses were chosen with the aid of a Smith chart using the wavelength of the dominant mode of the given excitation. Table I shows a listing of the first two initial guesses, optimized distances, and computed stub lengths for both mismatch cases. Only one significant digit was retained due to etching resolution of 0.005 in (0.127 mm). The absorbed and forward powers $\mathrm{P_L}$ and $\mathrm{P_f}$ were calculated from the source excitations and source and load admittances [14]

$$\mathrm{P_L} = \boldsymbol{v}_{\rm m}(z)^* \cdot \boldsymbol{Y}_{\rm in}^{\rm m}(z) \cdot \boldsymbol{v}_{\rm m}(z) \tag{17a}$$

$$\mathrm{P_f} = \boldsymbol{v}_{\rm m}(z)^* \cdot \left(\left[\mathbf{1}_n + \boldsymbol{\Gamma}_{\rm in}^{\rm m}(z)\right]^{-1}\right)^* \cdot \boldsymbol{Y}_{\rm ch}^{\rm m}\left[\mathbf{1}_n + \boldsymbol{\Gamma}_{\rm in}^{\rm m}(z)\right]^{-1} \cdot \boldsymbol{v}_{\rm m}(z) \tag{17b}$$

where $*$ denotes the complex conjugate transpose. For the matched case, (17a) and (17b) are evaluated at $z = -d$; for the unmatched case, $z = 0$.

The "short" mismatch (with parameter $d = 7.3$ mm) is superior since its d is one-half that of the "open" case. Calculations using the simulated transformation matrix show that the matching network significantly reduces the self-mode and intermode voltage reflections. Fig. 3 shows these simulated self-mode reflections as functions of frequency. The phase response clearly indicates the difference in modal propagation constants. Reflections clearly are minimized 2.0 GHz.

The mutual matching strategy was applied to a mismatched load where nearest neighbors were "shorted" with 26 Ω ($[\boldsymbol{\mathcal{Z}}_{\rm L}]_{12,\,21,\,23,\,32} = 26\ \Omega$) from their characteristic admittance-derived value of 287 Ω. Three solutions sets were found

TABLE I
OPTIMIZED MATCHING NETWORK PARAMETERS

Solution Set	$z = -d_{\rm guess}$ (mm)	$z = d$ (mm)	l or X	$\boldsymbol{V}_{\rm S}$ (V)	$\mathrm{P_f}$ w/o match	$\mathrm{P_L}$ w/o match	$\mathrm{P_f}$ with match	$\mathrm{P_L}$ with match
Outer line "Open" mismatch with stub match								
1	14.2 ($\frac{3}{16}\lambda$)	13.9	25.6 mm	(1,1,1)	7.46	5.42	7.34	7.32
2	23.7 ($\frac{5}{16}\lambda$)	26.9	12.0 mm	(1,1,1)	7.46	5.42	7.45	7.15
Outer line "Short" mismatch with stub match								
1	4.7 ($\frac{1}{16}\lambda$)	7.3	10.5 mm	(1,1,1)	6.96	5.78	7.38	7.36
2	33.2 ($\frac{7}{16}\lambda$)	33.3	27.4 mm	(1,1,1)	6.96	5.78	7.56	7.45
Mutual mismatch "short" with interline reactance match								
1	4.0	8.14	0.90 pF	(0,1,0)	2.64	1.77	2.50	2.37
7	28.0	51.88	0.88 pF	(0,1,0)	2.65	1.84	2.49	2.33
8	32.0	35.60	0.15 nH	(0,1,0)	2.62	1.80	2.50	2.42
Mutual mismatch "short" with interline center-tune match								
1	2.0	6.1	1.19 pF	(0,1,0)	2.49	1.71	2.47	2.47
7	14.0	37.0	0.18 nH	(0,1,0)	2.53	1.75	2.48	2.48
9	18.0	49.2	1.21 pF	(0,1,0)	2.47	1.75	2.47	2.46
Amplifier mismatch termination with interline reactance match								
1	8.0	48.0	0.14 pF	(0,1,0)	2.59	1.56	2.53	1.36
Amplifier termination, interline center-tune match								
3	6.0	55.6	0.21 nH	(0,1,0)	2.23	1.55	2.62	2.16
5	10.0	26.5	1.45 pF	(0,1,0)	2.57	1.37	2.72	2.07
6	12.0	15.1	0.25 nH	(0,1,0)	2.41	1.30	2.66	2.09
Amplifier termination with quarter-wave transformer match								
1	-	-	-	(0,1,0)	2.51	1.63	2.45	2.06

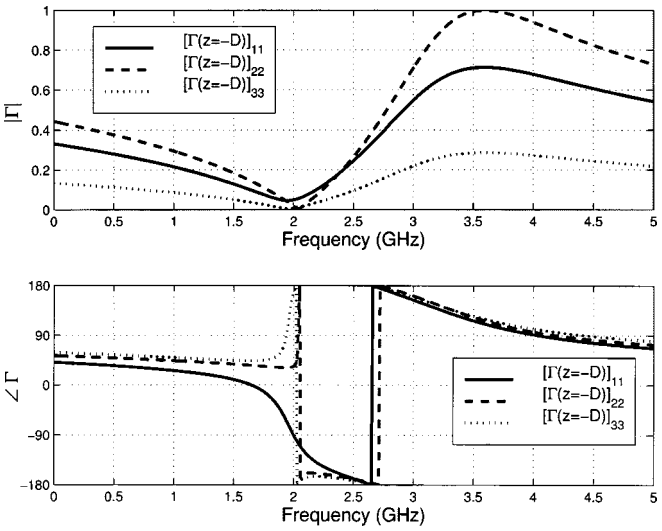

Fig. 3. Simulated mode reflection-coefficient variation over frequency for mode self-reflection terms $[\boldsymbol{\Gamma}_{\rm L}^{\rm m}(z = -D)]_{11}$, $[\boldsymbol{\Gamma}_{\rm L}^{\rm m}(z = -D)]_{22}$, $[\boldsymbol{\Gamma}_{\rm m}(z = -D)]_{33}$. Stubs optimized for 2.0 GHz with open on termination elements $[\boldsymbol{Z}_{\rm L}^{\rm Y}]_{11}$ and $[\boldsymbol{Z}_{\rm L}^{\rm Y}]_{33}$: $d = 7.32$ mm, $l = 10.58$ mm.

to increase the absorbed power in the three cases by an average of 28%. Again, parameters and full power relations are shown in Table I. The "center tune" match, however, increases the absorbed power by an average of 30% and almost perfectly matches this "short." Three solutions using (15) were obtained.

Both interline reactance match criteria [see (14) and (15)] were also tested on a more sophisticated "amplifier" termination, for which $[\boldsymbol{\mathcal{Z}}_{\rm L}]_{22} \approx 20\ {\rm k}\Omega$, $[\boldsymbol{\mathcal{Z}}_{\rm L}]_{12,\,21,\,23,\,32} \approx 500\ \Omega$, and $[\boldsymbol{\mathcal{Z}}_{\rm L}]_{13,\,31} \approx 10\ {\rm k}\Omega$. Such a termination could be encountered in a transistor amplifier application. Match (14) actually increased the mismatch. However, the "center tune" interline reactance increased absorbed power 12%–25%, with better matching for smaller d (see Table I for complete power relations and parameters).

Finally, the quarter-wave transformer strategy was tested on a mismatch. The nonlinear equation (16) is generally difficult to solve when information about $\boldsymbol{Y}_q$ is not known *a priori*. However, reciprocity guarantees symmetric matrices, and symmetry about the $x = 0$ plane reduces the independent variables to four since the matrix is symmetric across the opposite diagonal. Thus, four nonlinear equations (quadratic with respect to each variable independently) arise from (16). These may be easily solved using *Mathematica*.[1] For one simulation, eight total solutions were obtained, but four were immediately discarded due to nonphysical negative terms in the impedance matrix; the remaining three violated the dominance condition on the realizable admittance matrix [18]. One solution for an "amplifier" type of termination with $[\boldsymbol{\mathcal{Z}}_{\rm L}]_{22} \approx 2\ {\rm k}\Omega$ was obtained; line 2 was narrowed in several iterations and an average increase of 19% absorbed power resulted.

In all cases, calculation of power absorption verified the effectiveness of the matching networks. In Table I, the forward-traveling power $P_{\rm f}$ and power absorbed the load (assuming the lines and matching networks are lossless) $P_{\rm L}$ demonstrate the matching. Certain solution sets were repeated for various initial guesses and, therefore, have been omitted. In nearly all cases, the matching solutions nearer to $z = 0$ resulted in greater absorbed power, as the effect of the mode delays decreased with smaller coupling lengths.

Each matching network solution was checked using Agilent's Advanced Design System. All powers were verified with under 1% error; these resulted from termination value truncations and substrate approximations.

V. Calibration and Measurement Results

To demonstrate the validity of the matching strategies, several three-coupled microstrip structures were constructed. We fabricated Fig. 2 for the stub-corrected "short" mismatch (solution 1: $d = 7.3$ mm, $l = 10.5$ mm) on Kepro FR-4 circuit boards using the dimensions given in Section IV. Tight physical coupling between lines precluded adjacent connectors in Fig. 2. Thus, the coupled lines were accessed with fan-ins and fan-outs, as shown in Fig. 4. Lines 1 and 3 were angled 20° from the z-axis and continued 17.58 mm from the reference planes to the board edges. SMA flange mount connectors (female 3.5-mm coaxial cable to microstrip tab adapter) were then soldered directly to the lines

[1]Wolfram Research Inc., Champaign, IL, 1991.

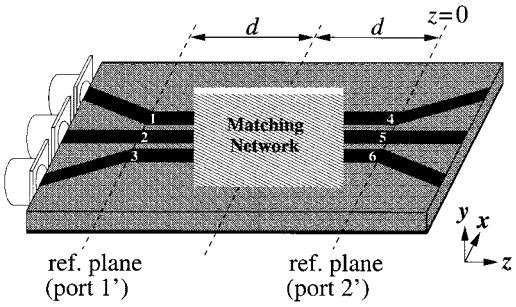

Fig. 4. Device-under-test, with input and output sections, reference planes, and SMA connectors.

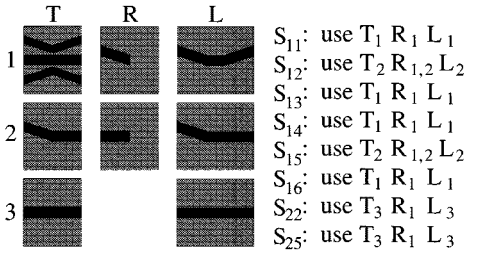

Fig. 5. TRL standards used in measurement for the conductor S-parameter measurements. The independent S-parameters are listed along with required standards for their respective measurements.

at these edges. The bend discontinuity suffered a simulated mismatch of no greater than 52 Ω; in fact, the worst discontinuity measured via time-domain reflectometry (TDR) was 55 Ω from a poor solder connection. We then calculated the conductor and mode reflection-coefficient matrices from the measured (6 × 6) conductor and mode S-parameter description of the coupled lines, performed on an HP 84510C automatic network analyzer (ANA). Identical SMA connectors and solder joints were also used for both the unknowns and calibration standards.

For the modal S-parameters, we employed the multimode multiconductor transmission line (MMTRL) algorithm [19], which converts conductor S-parameter measurements to modal measurements. This algorithm requires three necessary standards (thru, reflect, and line) with the same fan-in and fan-out sections as the unknown, using identical board material and chemical etching process. However, the conductor measurements required a renormalization algorithm [20] to combine two-port measurements into the final (6 × 6) S-parameters. Symmetry and reciprocity (as in Fig. 2) reduce the number of independent S-parameters to 13. Furthermore, if $D = 2d$ in Fig. 2 (as in our case), only eight measurements are required, i.e., S_{11}, S_{12}, S_{13}, S_{14}, S_{15}, S_{16}, S_{22}, and S_{25}.

For the conductor S-parameters, we used a hybrid "two-tier" calibration. First, a short-open-load-termination (SOLT) calibration deembedded the test cables. To proceed with the measurement, we needed eight distinct TRL calibrations to deembed the appropriate fan-in and fan-out sections individually. For example, to measure S_{11} and S_{14}, we calibrated through the microstrip–coax junction and the angled sections attached to ports 1 and 4. We used fabricated standards T_1, R_1, and L_1, as shown in Fig. 5, in accordance with the common thru-reflect-line (TRL) calibration [21]. Note that only the top line in the standard T_1 was used; this was also the thru standard

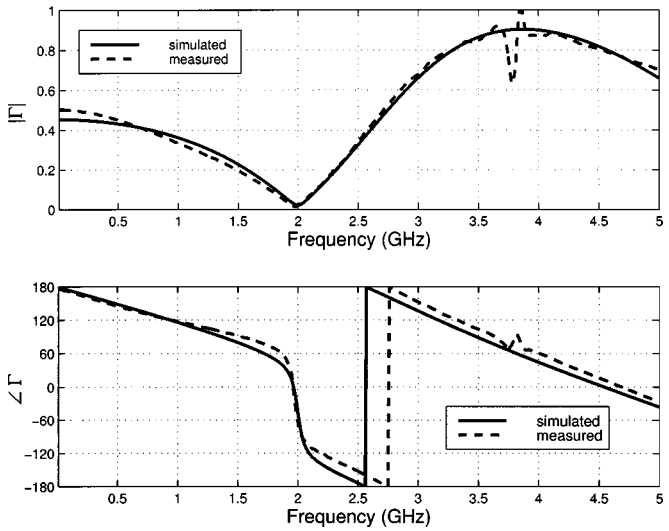

Fig. 6. Comparison of measured and simulated frequency variation for line self-reflection terms $[\mathbf{\Gamma}_{\mathrm{L}}^{\mathrm{c}}]_{11,33}$ at $z = -21.1$ mm with "short" mismatch corrected by stubs.

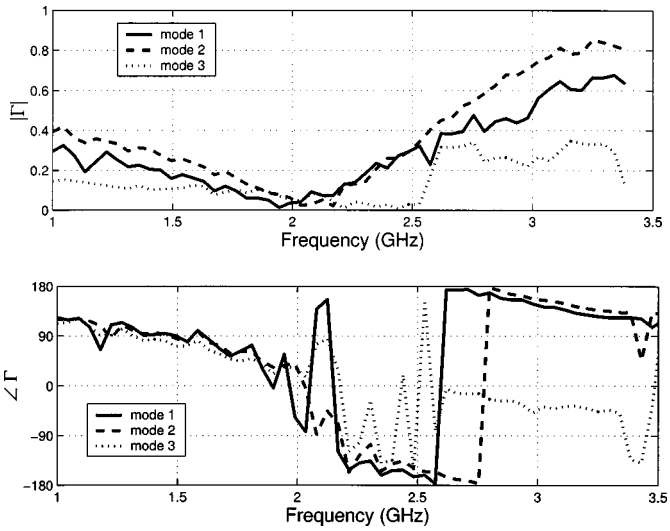

Fig. 7. Measured mode reflection-coefficient variation over frequency for mode self-reflection terms $[\mathbf{\Gamma}_{\mathrm{L}}^{\mathrm{m}}(z = -D)]_{11}$, $[\mathbf{\Gamma}_{\mathrm{L}}^{\mathrm{m}}(z = -D)]_{22}$, $[\mathbf{\Gamma}_{\mathrm{m}}(z = -D)]_{33}$. Stubs optimized for 2.0 GHz with open on termination elements $[Z_{\mathrm{L}}^{\mathrm{Y}}]_{11}$ and $[Z_{\mathrm{L}}^{\mathrm{Y}}]_{33}$: $d = 7.32$ mm, $l = 10.58$ mm.

used for the MMTRL, as we had no substitute angled-to-angled line thru isolated from the other lines. The remainder of the independent measurements used various combinations from the remainder of the eight standards, as listed in Fig. 5. Thus, the total calibration involved four distinct TRL calibrations and established reference planes at coupled-line system inputs labeled in Fig. 4. Clearly, the major source of error in this calibration procedure is its failure to account for coupling between the lines in the fan-ins and fan-outs (no adjacent lines). We expected this to be especially problematic close to the reference planes and for high frequencies. The eight independent S-parameters obtained from these calibrations fully characterize the structure in Fig. 2. Though some of the calibrations yielded redundant measurements (e.g., S_{44}), these provided an understanding of the symmetry limitations, which were tangible, but for our purposes, negligible. The TRL coefficients for each calibration configuration were calculated in software and graphically examined to save time in repeating measurements altered by bad connections, though connections were shown to be repeatable. More importantly, this process revealed resonance frequencies in certain thru and line calibration standard fixtures (one of which was the MMTRL thru), which altered results at certain frequencies.

Using the complete conductor and mode S-parameter matrices, referenced as per Fig. 4, we computed both (3×3) conductor and mode input reflection-coefficient matrices $\mathbf{\Gamma}_{\mathrm{in}}^{\mathrm{c}}$ and $\mathbf{\Gamma}_{\mathrm{in}}^{\mathrm{m}}$ seen by the source ($z = -D$) for prescribed load terminations $\mathbf{\Gamma}_{\mathrm{L}}^{\mathrm{c}}$ or $\mathbf{\Gamma}_{\mathrm{L}}^{\mathrm{m}}$ for the mismatched termination network corresponding to the "short." For both conductor and mode quantities, we have

$$\mathbf{\Gamma}_{\mathrm{in}} = [\boldsymbol{S}]_{11} + [\boldsymbol{S}]_{12} \cdot \left([\mathbf{\Gamma}_{\mathrm{L}}]^{-1} - [\boldsymbol{S}]_{22}\right)^{-1} \cdot [\boldsymbol{S}]_{21} \qquad (18)$$

where $\boldsymbol{S}$ is the measured (6×6) S-parameter matrix and $[\boldsymbol{S}]_{ij}$ are its (3×3) submatrices. Matrix $\mathbf{\Gamma}_{\mathrm{L}}$ accounts for the load mismatch at port $2'$ (the load in Fig. 2) and is calculated from (4).

Matrices $\boldsymbol{Y}_{\mathrm{ch}}^{\mathrm{m}}$ and $\boldsymbol{Y}_{\mathrm{ch}}^{\mathrm{c}}$ were the only quantities not directly measured. Instead we used their numerical approximations (generated using ***RLGC*** and verified with other quasi-static methods) from the synthesis simulations. Results were negligibly sensitive to this approximation.

Good correlation between the simulated and measured $\mathbf{\Gamma}_{\mathrm{in}}^{\mathrm{c}}(z = -D)$ results is observed in Fig. 6. Reflection minimization at 2.0 GHz demonstrates that reflected power can be almost eliminated for the simple mismatch cases. The disturbance at 3.8 GHz in Fig. 6 represents one of the resonant frequencies encountered for the MMTRL thru), which had adjacent feedlines for which we had no available substitute. Measured phase followed the general trend, with deviation mainly confined to dc and high-frequency regions. The major assumptions concerned consistent solder connections, a consistent TRL standard substrate, and matched terminations.

Finally, the MMTRL measured mode reflection coefficients as per (18). Results are shown in Fig. 7 and agree well with the simulated values shown in Fig. 3. Only mode 3 suffered from significant error due to the sensitivity of this mode's small reflections. These resulted from its field configuration, where a concentration of field energy between the center and outer lines negates the effects of the stubs. Extracted propagation constants were compared to our simulated quasi-TEM values (generated from ***RLGC***). Phase constants are shown in Fig. 8, and clearly agree with the quasi-TEM values with acceptable error.

Several structures incorporating the interline reactance matching networks for mutual mismatches were also fabricated. Measurements are currently being conducted and will be presented in the future. The quarter-wave transformer should be expected to yield similar, though less significant matching, as observed in simulations (see Table I). For now, the main goal of validating one of the matching networks (tuning stubs) has been accomplished and the stub strategy would clearly be applicable to transistor amplifiers or coupled-line bus systems with mismatched drivers on the outer lines.

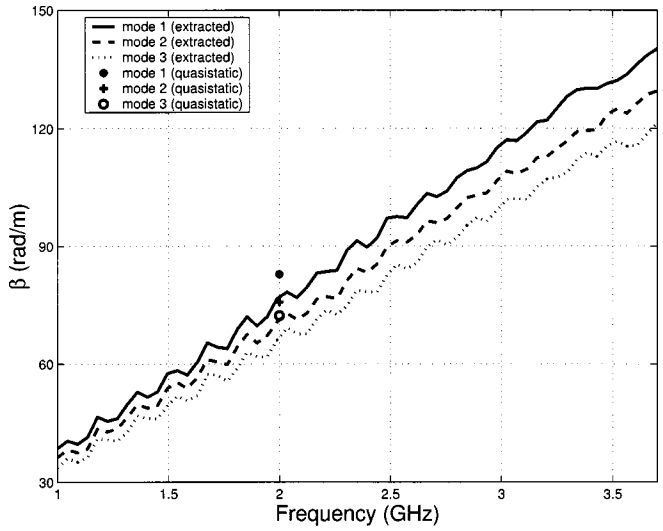

Fig. 8. Measured phase constants from the MMTRL algorithm compared with ***RLGC***-simulated values at 2.0 GHz.

VI. Conclusions

We have introduced several new matching techniques for a coupled-microstrip structures. Practical applications will certainly include more complicated mismatches and greater coupling lengths for which our detailed matching methods may be individually less effective. However, the main goal was validation of the techniques, made possible through frequency-domain measurements. Certainly, more extensive measurements and more precise calibration procedures are under consideration. Currently, we have no alternative conductor S-parameter calibration, but perhaps measurements and optimization of the MMTRL thru will allow S-parameter extraction of its cascaded sections. Finally, the calibration and measurement assumptions warrant an error analysis.

Future work includes combination of these methods, hybridization with other methods, and development of better optimization procedures. Specifically, optimization of power functions given the excitations and boundary conditions will alleviate the dominant-mode concern and the voltage–wave matching approach, thereby bilaterally "matching" to achieve desired maximum power transfer to the load. Also, parallel stubs and other novel structures with possible matching capability should be investigated. Finally, full EM modeling will improve the discontinuity models and other significant effects arising with increasing application frequencies.

Acknowledgment

The authors wish to acknowledge Prof. P. Klock, Department of Electrical and Computer Engineering, University of Illinois at Urbana-Champaign, who suggested beneficial measurement tips and assisted with the HP automation software, Prof. A. Cangellaris, Department of Electrical and Computer Engineering, University of Illinois at Urbana-Champaign, who provided theoretical assistance and guidance, and K. Coperich, Department of Electrical and Computer Engineering, University of Illinois at Urbana-Champaign, who offered much advice and encouragement.

References

[1] K. D. Marx, "Propagation modes, equivalent circuits, and characteristic terminations for multiconductor transmission lines with inhomogeneous dielectrics," *IEEE Trans. Microwave Theory Tech.*, vol. MTT-21, pp. 450–457, July 1973.

[2] C. R. Paul, "Decoupling the multiconductor transmission line equations," *IEEE Trans. Microwave Theory Tech.*, vol. 44, pp. 1429–1440, Aug. 1996.

[3] D. F. Williams, L. A. Hayden, and R. B. Marks, "A complete multimode equivalent-circuit theory for electrical design," *J. Res. Natl. Bur. Stand.*, pp. 405–423, Aug. 1997.

[4] J. T. Kuo and C. H. Tzuang, "A termination scheme for high-speed pulse propagation on a system of tightly coupled coplanar strips," *IEEE Trans. Microwave Theory Tech.*, vol. 42, pp. 1008–1015, June 1994.

[5] S. Amari and J. Bornemann, "Optimum termination networks for tightly coupled microstrip lines under random and deterministic excitations," *IEEE Trans. Microwave Theory Tech.*, vol. 45, pp. 1785–1789, Oct. 1997.

[6] J. E. Schutt-Aine and R. Mittra, "Analysis of pulse propagation in coupled transmission lines," *IEEE Trans. Circuits Syst. I*, vol. CAS-32, pp. 1214–1219, Dec. 1985.

[7] ——, "Nonlinear transient analysis of coupled transmission lines," *IEEE Trans. Circuits Syst. I*, vol. 36, pp. 959–966, July 1989.

[8] G. T. Lei, G. W. Pan, and B. K. Gilbert, "Examination, clarification, and simplification of modal decoupling method for multiconductor transmission lines," *IEEE Trans. Microwave Theory Tech.*, vol. 43, pp. 2090–2100, Sept. 1995.

[9] K. Reiss and O. A. Palusinski, "Procedure for direct calculation of characteristic admittance matrix of coupled transmission lines," *IEEE Trans. Microwave Theory Tech.*, vol. 44, pp. 152–154, Jan. 1996.

[10] G. C. Gentili and M. Salazar-Palma, "The definition and computation of modal characteristic in quasi-TEM coupled transmission lines," *IEEE Trans. Microwave Theory Tech.*, vol. 43, pp. 338–343, Feb. 1995.

[11] Y.-Y. Sun, "On multiconductor quarter-wave matching section," *J. Chinese Inst. Eng.*, vol. 3, pp. 147–152, 1980.

[12] V. K. Tripathi, "On the analysis of symmetrical three-line microstrip circuits," *IEEE Trans. Microwave Theory Tech.*, pp. 726–729, Sept. 1977.

[13] G. E. Ponchak and L. P. B. Katehi, "Open- and short-circuit terminated series stubs in finite-width coplanar waveguide on silicon," *IEEE Trans. Microwave Theory Tech.*, vol. 45, pp. 970–976, June 1997.

[14] J. G. Nickel and J. E. Schutt-Aine, "Investigation of the longitudinal multiconductor transmission line functions for symmetric coupled-microstrip systems," *IEEE Trans. Microwave Theory Tech.*, vol. 50, pp. 183–190, Jan. 2002.

[15] ——, "Several narrowband matching networks for quasi-TEM coupled microstrip lines," in *IEEE 9th Topical Elect. Performance Electron. Packag. Meeting*, Oct. 2000, pp. 296–299.

[16] K. S. Oh, D. B. Kuznetsov, and J. E. Schutt-Aine, "Capacitance computations in a multilayered dielectric medium using closed-form spatial Green's functions," *IEEE Trans. Microwave Theory Tech.*, vol. 42, pp. 1443–1453, Aug. 1994.

[17] K. G. Gupta, R. Garg, and R. Ghadha, *Computer-Aided Design of Microwave Circuits*. Norwood, MA: Artech House, 1981.

[18] L. Weinberg, *Network Analysis and Synthesis*. New York: McGraw-Hill, 1962.

[19] C. Seguinot, J.-F. Legier, F. Huret, E. Paleczny, and L. Hayden, "Multimode TRL—A new concept in microwave measurements: Theory and experimental verification," *IEEE Trans. Microwave Theory Tech.*, pp. 536–542, May 1998.

[20] S. Sercu and L. Martens, "Characterizing n-port packages and interconnections with a 2-port network analyzer," *Elect. Performance Electron. Packag.*, pp. 163–166, 1997.

[21] G. F. Engen and C. A. Hoer, "Thru-reflect-line: An improved technique for calibrating the dual six-port automatic network analyzer," *IEEE Trans. Microwave Theory Tech.*, vol. MTT-27, pp. 987–993, Dec. 1979.

Josh G. Nickel (S'95) was born on November 27, 1974, in Lancaster, PA. He received the B.S. degree (with honors) in electrical engineering from the Pennsylvania State University, University Park, in 1997, and the M.S. and Ph.D. degrees in electrical engineering from the University of Illinois at Urbana-Champaign, in 1999 and 2001, respectively.

From 1997 to 2001, he was a Research Assistant with the Center for Computational Electromagnetics, University of Illinois at Urbana-Champaign, and was a Teaching Assistant in automated microwave measurements for six semesters. He assisted in the construction of a 16-processor parallel Linux cluster or "Beowulf" supercomputer. He has held internships at AMP Inc., the MITRE Corporation, IBM, and SAIC/Demaco. He is currently with Silicon Bandwidth Inc., Fremont, CA. His current research interests are in packaging and multiconductor transmission-line simulation and analysis.

Mark D. Hampson was born on October 1, 1980, in Hoffman Estates, IL. He is currently working toward the B.S. degree in electrical engineering at the University of Illinois at Urbana-Champaign.

He is with Xindium Technologies Inc., Champaign, IL, on a part-time basis.

Ho-Young R. Chung was born on July 21, 1979, in Peoria, IL. He received the B.S. degree in electrical engineering from the University of Illinois at Urbana-Champaign, in 2001.

He currently with Raytheon Inc., El Segundo, CA, where he is involved with RF systems.

José E. Schutt-Ainé (S'86–M'86–SM'98) received the B.S. degree from the Massachusetts Institute of Technology (MIT), Cambridge, in 1981, and the M.S. and Ph.D. degrees from the University of Illinois at Urbana-Champaign (UIUC), in 1984 and 1988, respectively.

From 1981 to 1983, he was an Application Egineer at the Hewlett-Packard Microwave Technology Center, Santa Rosa, CA, where he was involved with transistor modeling. He held summer positions at GTE Network Systems, Northlake, IL during his graduate studies. In 1989, he joined the faculty of the Electromagnetic Communication Laboratory, UIUC, where he is currently an Associate Professor of electrical and computer engineering. His interests include microwave theory and measurements, electromagnetics, high-frequency circuit design, and electronic packaging.